

Scaling of locally averaged energy dissipation and enstrophy density in isotropic turbulence

Kartik P Iyer¹, Jörg Schumacher^{1,2}, Katepalli R Sreenivasan³,
P K Yeung⁴

¹Department of Mechanical and Aerospace Engineering, New York University, New York, NY, 11201, USA

²Institut für Thermo-und Fluidodynamik, Technische Universität Ilmenau, Postfach 100565, D-98684 Ilmenau, Germany

³Institute for Advanced Study, Princeton, NJ 08540

⁴School of Aerospace Engineering and Mechanical Engineering, Georgia Institute of Technology, Atlanta, GA 30332, USA

E-mail: kartik.iyer@nyu.edu

Abstract. Using direct numerical simulations of isotropic turbulence in periodic cubes of several sizes, the largest being 8192^3 yielding a microscale Reynolds number of 1300, we study the properties of pressure Laplacian to understand differences in the inertial range scaling of enstrophy density and energy dissipation. Even though the pressure Laplacian is the difference between two highly intermittent quantities, it is non-intermittent and essentially follows Kolmogorov scaling, at least for low-order moments. Using this property, we show that the scaling exponents of local averages of dissipation and enstrophy remain unequal at all finite Reynolds numbers, though there appears to be a *very* weak tendency for this inequality to decrease with increasing Reynolds number.

Keywords: local averaging, scaling, enstrophy, dissipation, pressure laplacian
Submitted to: *New J. Phys.*

As in other highly correlated systems [1, 2], “local” averaging over scales smaller than the system size is often employed [3, 4] in turbulence to study its statistical structure. Local averages of highly intermittent quantities are dependent on the averaging scale itself [5, 6, 7] and paradigms such as the central limit theorem do not apply. Properties of local averages of energy dissipation [8] (characterizing straining motions) and enstrophy [9] (characterizing local rotation) are the subject of much debate. The consensus of experimental and numerical work is that the local averages of these two quantities are different [10, 11, 12, 13, 14, 15, 16] while theories (with some numerical support), rooted in the paradigm of small-scale universality [17, 18, 19, 20, 21, 22], conclude oppositely.

Here, we reconcile this difference by establishing two specific results. First, we show that the pressure Laplacian, which engenders the topological asymmetry between dissipation and enstrophy [23, 24, 13, 25], assumes a nearly self-similar (i.e., non-intermittent) form in the inertial range (IR); even though the pressure Laplacian is the difference between two highly intermittent quantities, it is non-intermittent and essentially follows Kolmogorov scaling. Second, while the pressure [26, 27, 28] does constrain the scaling of local averages of dissipation and enstrophy, the self-similar property of the pressure Laplacian implies that the exponents remain unequal at all finite Reynolds numbers, though this constraint appears to weaken very slowly with increasing Reynolds number.

Direct Numerical Simulations: We use a direct numerical simulation (DNS) database of isotropic turbulence obtained by solving the incompressible, three-dimensional Navier-Stokes equations or the components of the turbulent velocity field $u_i(\mathbf{x}, t)$ with $i = x, y, z$ in a periodic cube with edge length $L_0 = 2\pi$, spanning a wide range of Reynolds numbers [29]. Taylor microscale Reynolds numbers up to 1300 were used. The largest DNS was conducted on a grid size of 8192^3 [22]. A statistically steady state was obtained by forcing the low Fourier modes [29]. Averages over ten large-eddy turnover times were used for the analysis; $\langle \cdot \rangle$ denotes space/time averages.

Definitions. It is well known in homogeneous turbulence that $\epsilon = \Omega + 2\nu(\partial u_i/\partial x_j \partial u_j/\partial x_i)$, where $\epsilon \equiv \frac{\nu}{2}(\partial u_i/\partial x_j + \partial u_j/\partial x_i)^2$ is the turbulent energy dissipation rate per unit mass, ν is the kinematic viscosity of the fluid and the summation convention is implied; the enstrophy density is given by $\Omega \equiv \nu|\omega|^2$, where $\omega = \nabla \times \mathbf{u}$ is the vorticity.

Define the local average of dissipation and enstrophy at scale r as,

$$\epsilon_r(\mathbf{x}, t) = \frac{1}{V_r} \int_{V_r} \epsilon(\mathbf{x} + \mathbf{x}', t) d\mathbf{x}', \quad \Omega_r(\mathbf{x}, t) = \frac{1}{V_r} \int_{V_r} \Omega(\mathbf{x} + \mathbf{x}', t) d\mathbf{x}', \quad (1)$$

where $V_r = r^3$ is a volume centered around \mathbf{x} . Taking the divergence of the Navier-Stokes equations at constant mass density ρ_0 , we obtain the Poisson equation for the pressure field p , which can then be related via its Laplacian to ϵ and Ω as $\Omega = \epsilon + 2\nu\Delta p/\rho_0$. Averaging this relation over volume of scale $r \geq 0$, we get

$$\Omega_r(\mathbf{x}, t) = \epsilon_r(\mathbf{x}, t) + (2\nu/\rho_0)\Delta p_r(\mathbf{x}, t), \quad (2)$$

where Δp_r is the locally averaged field of the pressure Laplacian Δp over scale r and is given by the surface integral, in accordance with Gauss's theorem, as

$$\Delta p_r(\mathbf{x}, t) \equiv \frac{2\nu\rho_0}{V_r} \int_{s_r} \frac{\partial}{\partial x_j} u_i(\mathbf{x} + \mathbf{x}', t) u_j(\mathbf{x} + \mathbf{x}', t) ds_i. \quad (3)$$

Here, s_r denotes the surface around volume V_r . For brevity, in what follows, we drop the dependence on (\mathbf{x}, t) : for instance, $\epsilon_r \equiv \epsilon_r(\mathbf{x}, t)$. We note that in homogeneous turbulence, for any $r \geq 0$, $\langle \Delta p_r \rangle = 0$ or equivalently, $\langle \epsilon_r \rangle = \langle \Omega_r \rangle$. But higher moments of ϵ_r and Ω_r can differ.

Results. To build up some intuition, we show in Fig. 1 all three fields in a small sub-volume of the computational box, coarse grained with respect to scale r . The

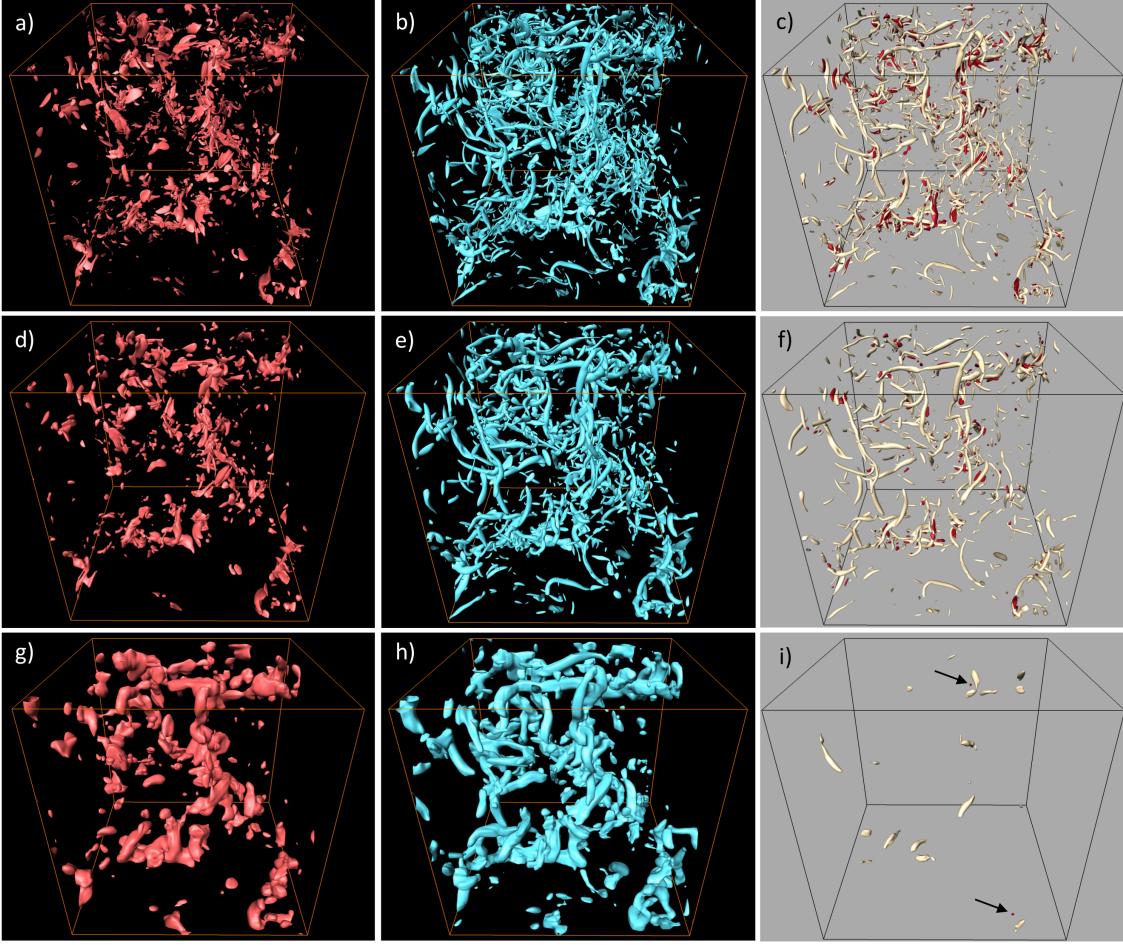


Figure 1. Isosurface plots of the kinetic energy dissipation rate (a,d,g), the local enstrophy (b,e,h), and the pressure Laplacian (c,f,i). Data are obtained from the DNS at the highest Reynolds number in a cubic sub-volume with a side length $L_0/16$. Panels (a,b,c) show the data without spatial averaging at an isosurface level of 1.5 in characteristic units of the DNS. Panels (d,e,f) display the fields for $r = 10\eta$ at a level of 1.0; $\eta = (\nu^3/\langle\epsilon\rangle)^{1/4}$ is the Kolmogorov length of the flow. Panels (g,h,i) display the field at $r = 33\eta$ at a level of 0.5. Positive isosurfaces for the pressure Laplacian are shown in yellow and negative ones in red, in panels (c,f,i). In panel (i) negative contours are indicated by black arrows.

top row shows quantities without any averaging while the bottom two rows are locally averaged quantities for two averaging scales r and two different thresholds. The top row displays the typical structure: while the dissipation layers appear more sheet-like, maxima of the local enstrophy are tube-like [9, 22]. This is a fingerprint of the local vortex-stretching, a central building block of three-dimensional turbulence. High-amplitude shear layers (leading to dissipation) are the result of self-induced strain and result in ongoing stretching [30, 31]. With increasing r , the differences between ϵ_r and Ω_r become less consequential, as the panels (f) and (i) show. Panels (c), (f) and (i) show that the local pressure Laplacian isosurfaces of positive amplitude appear to have a spatial correlation with local enstrophy. Pressure minima or pressure Laplacian

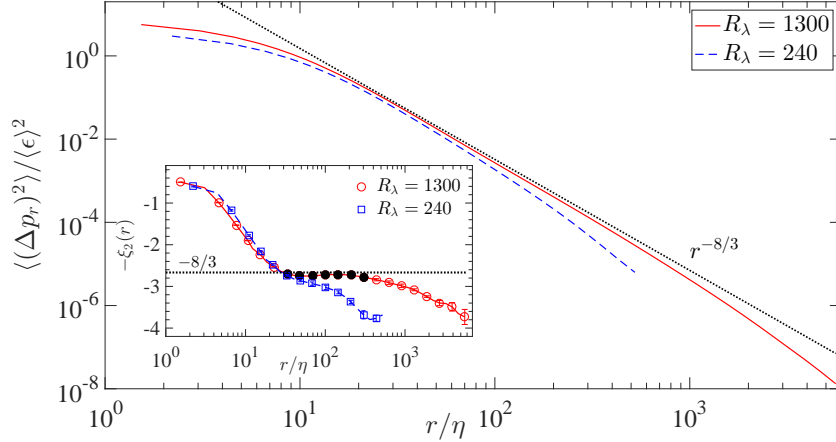


Figure 2. Variance of the locally averaged pressure Laplacian as a function of the averaging scale r . Dashed line corresponds to the Kolmogorov mean-field [32] scaling of $r^{-8/3}$. Inset shows the exponent $\xi_2(r) = d[\log\langle(\Delta p_r)^2\rangle]/d[\log r]$ vs. r/η . The dotted line corresponds to the self-similar exponent, $\xi_2 = 8/3$. The IR, $r/\eta \in (25, 350)$ for $R_\lambda = 1300$, is marked by (\bullet).

maxima are found in the low dissipation vortex cores beyond which Δp_r and ϵ_r tend to be positively correlated, since positive local pressure Laplacian isosurfaces have a greater correspondence with local dissipation at larger scales (compare panels (f,i) with (d,g), respectively), in relation to that at the smallest scales (compare panel (c) with (a)). The pressure Laplacian isosurfaces of negative amplitude (but same magnitude) are much more sparsely distributed indicating a positively skewed field.

By examining the variance, skewness and flatness of the pressure Laplacian Δp_r , we now show that it has attributes of self-similar Kolmogorov-like scaling at high Reynolds numbers. First, Fig. 2 shows that the variance of Δp_r in IR ($\eta \ll r \ll L$) follows the power-law, $\langle(\Delta p_r)^2\rangle \sim r^{-\xi_2}$ where ξ_2 is the scaling exponents. Kolmogorov's arguments [32], which do not account for intermittency, imply that $\xi_2 = 8/3$; the measured second-order exponent is quite close (see the inset which presents local slopes), with the higher Reynolds number data showing better conformity. The trend towards intermittency-free scaling of $\langle(\Delta p_r)^2\rangle$ reported here is consistent with that of the Δp spectrum, reported in Refs. [33, 34].

Now, the condition for self-similarity is that the exponent, $\sigma_q := \xi_q/q$, where ξ_q is the scaling exponent of Δp_r at order q , should be a constant over a range of scales; for Kolmogorov scaling, this ratio must be $4/3$. In Fig. 3, we plot the local slopes for the second, third and fourth moments in this self-similar format for the highest Reynolds number considered. Although the behavior of the fourth order is less convincing than that of the second, there exists the tendency to the constant value of $4/3$ (within the error bars of σ_q), leading to the conclusion that Δp_r is likely to be a self-similar quantity following the Kolmogorov scaling at least at low orders; note, however, that the 4th moment of Δp_r is equivalent to the 12th moment for velocity differences [4]; this renders fourth-order statistics more sensitive to finite sampling effects, compared to lower orders.

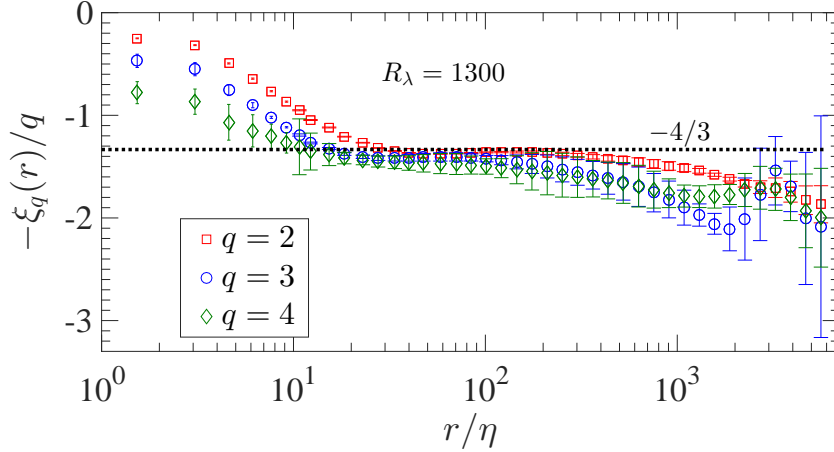


Figure 3. Quantities $\sigma_q := -\xi_q/q$ for $q = 2, 3$ and 4 , plotted against the averaging scale r for $R_\lambda = 1300$, where ξ_q is the scaling exponent of Δp_r at order q , $\langle (\Delta p_r)^q \rangle \sim r^{-\xi_q}$. The curves are close to the self-similar Kolmogorov value of $-4/3$ (dotted line) in IR. The error bars correspond to 95% confidence intervals obtained from temporal variations of the local slopes using a student's- t distribution.

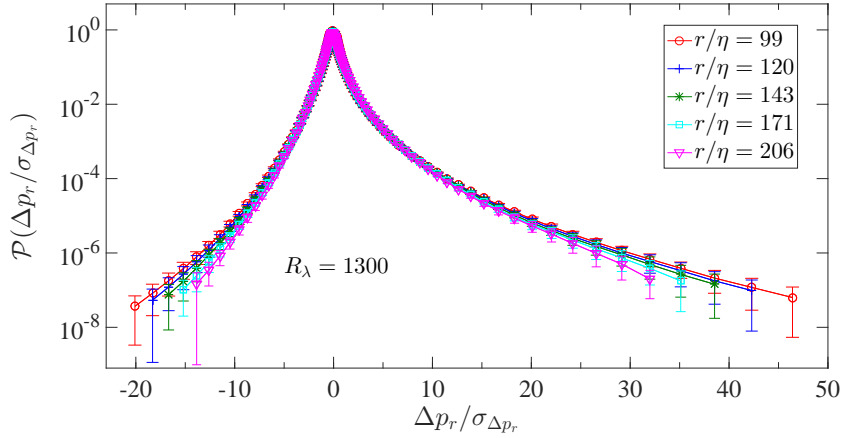


Figure 4. Probability density function (PDF) of the scale averaged pressure Laplacian Δp_r , normalized by its standard deviation, $\sigma_{\Delta p_r}$, at $R_\lambda = 1300$, for different IR separations. Error bars correspond to the standard deviation of $\mathcal{P}(\Delta p_r / \sigma_{\Delta p_r})$ over an ensemble of 16 temporal snapshots over 10 eddy turnover times. The PDFs collapse across the IR within error bars, demonstrating the self-similar nature of Δp_r .

Analogously, the probability density functions (PDFs) of Δp_r , normalized by the respective standard deviation, $\sigma_{\Delta p_r} = \langle (\Delta p_r)^2 \rangle^{1/2}$, collapse for different averaging scales r in the inertial range, as seen in Fig. 4, confirming that Δp_r is indeed self-similar. The PDF tails collapse within error bars, but less perfectly than the bulk, possibly due to finite sampling and finite Reynolds number effects. Furthermore, the PDFs are distinctly non-Gaussian and positively skewed. The skewness increases with Reynolds number, suggesting that high enstrophy and low dissipation events ($\Delta p_r > 0$), are increasingly more probable than the converse ($\Delta p_r < 0$), over inertial length scales.

If the skewness of Δp_r is positive, as can be seen visually in Fig. 1 and more quantitatively in Fig. 4, it follows that spatial averages of pressure Laplacian and

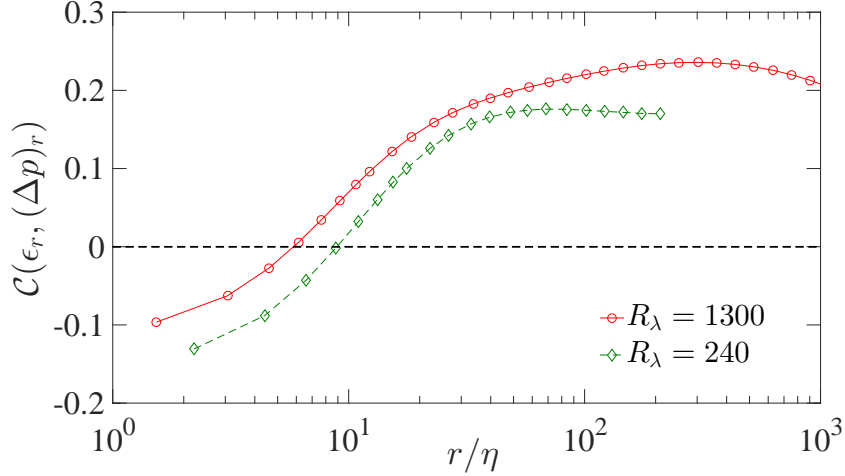


Figure 5. Correlation coefficient between scale averaged dissipation ϵ_r and scale averaged pressure Laplacian Δp_r , as a function of scale r . Dashed line at zero given for reference. For $r/\eta \gg 1$, $\langle \epsilon_r \Delta p_r \rangle > 0$ and increases with R_λ .

dissipation will be positively correlated. In fact, all $\langle \epsilon_r^m (\Delta p_r)^n \rangle > 0$ for $m \geq 1$ and $n \geq 1$ in the inertial range. Figure 5 shows, for the $m = n = 1$ case, the correlation coefficient, $\mathcal{C}(\epsilon_r, \Delta p_r) \equiv \langle \epsilon_r \Delta p_r \rangle / \sigma_{\epsilon_r} \sigma_{\Delta p_r}$. As $r/\eta \rightarrow 0$, $\langle \epsilon_r \Delta p_r \rangle < 0$, consistent with the picture that turbulence is comprised of low pressure (or high pressure Laplacian), high enstrophy vortex structures, wrapped around which are high dissipation sheets [35, 36, 25, 22]. When the averaging scale r increases, the average product $\langle \epsilon_r \Delta p_r \rangle$ eventually becomes positive since Δp_r is non-intermittent and remains positively skewed. Interestingly, the zeros of the two curves in Fig. 5 occur at about 6η and 8η for $R_\lambda = 1300$ and 240 , respectively; this is of the order of the characteristic scale that can be associated with the elementary Burgers vortex stretching mechanism, the Burgers radius, $r_B \approx 4\eta$ [37]. We find that the zero moves to smaller values as the Reynolds number increases and saturates at about 5η , which implies that the high-dissipation shear layer is wrapped as close as possible around the core of the stretched vortex filament at higher Reynolds numbers, $R_\lambda \gtrsim 1000$.

To see how the positivity of $\langle \epsilon_r^m (\Delta p_r)^n \rangle$ in the IR affects the exponents of scale-averaged dissipation and enstrophy, we average the q th power of both sides of Eq. 2 and get

$$\langle \Omega_r^q \rangle - \langle \epsilon_r^q \rangle = \langle (\Delta p_r)^q \rangle + \sum_{m=1}^{q-1} \frac{q!}{m!(q-m)!} \langle (\Delta p_r)^m \epsilon_r^{q-m} \rangle. \quad (4)$$

In IR, since $\langle (\Delta p_r)^q \rangle \geq 0$ and $\langle (\Delta p_r)^m \epsilon_r^n \rangle \geq 0$ for $m + n = q$, we conclude that $\langle \Omega_r^q \rangle \geq \langle \epsilon_r^q \rangle$. Now assume that ϵ_r and Ω_r follow a power law scaling in IR [38], $\langle \epsilon_r^q \rangle \sim r^{-\mu(q)}$ and $\langle \Omega_r^q \rangle \sim r^{-\tau(q)}$, where $\mu(q)$ and $\tau(q)$ are independent of R_λ for all r in the inertial range. It follows that

$$\tau(q) \geq \mu(q). \quad (5)$$

Figure 6 verifies this expectation for order $q = 2$, by showing the relative logarithmic derivative of $\langle \epsilon_r^2 \rangle$ with that of $\langle \Omega_r^2 \rangle$, at different R_λ . In the inertial range, the ratio

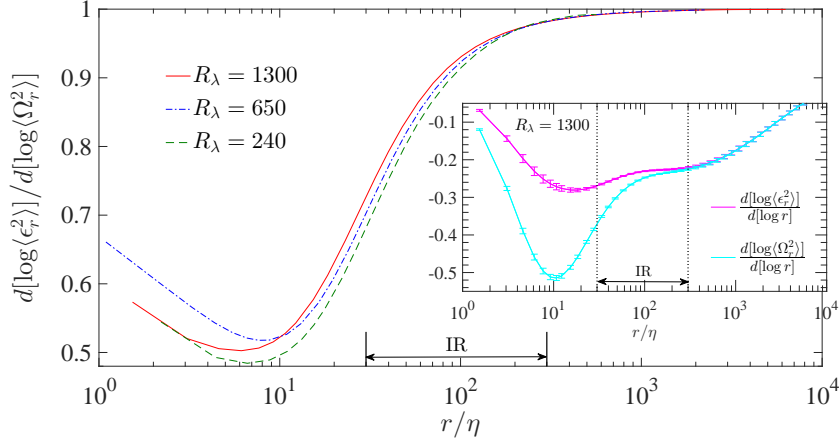


Figure 6. Logarithmic derivative of the second order local average of dissipation $\langle\epsilon_r^2\rangle$ with respect to second order local average of enstrophy $\langle\Omega_r^2\rangle$, as a function of the averaging scale r . The data show a very slow approach towards unity with R_λ in the inertial range. If the two scaling exponents have to be equal, the ordinate should be unity in IR (marked explicitly for the highest Reynolds number). The inset shows the local slopes of $\langle\epsilon_r^2\rangle$ and $\langle\Omega_r^2\rangle$ separately at $R_\lambda = 1300$, and shows that locally averaged dissipation scales better than locally averaged enstrophy in the IR. Error bars indicate 95% confidence intervals.

$\mu(2)/\tau(2) < 1$ for the Reynolds numbers examined, in agreement with Eq. 5. There appears to be a gradual trend towards unity but the trend appears to be extremely slow. We conclude that the inequality holds for all practical Reynolds numbers.

Conclusions: In the preceding sections, we have shown that the pressure Laplacian Δp_r , which is the difference of spatial averages of two highly intermittent quantities, namely the enstrophy which quantifies rotational motions and dissipation which characterizes the strain dominated motions, is a non-intermittent scale invariant quantity at high Reynolds numbers. This suggests that rotational and straining motions can be connected statistically in a relatively simple manner which is not order-dependent. Furthermore, we have established that the statistical asymmetry of Δp_r , results in the uni-directional ordering of the scaling exponents of the moments $\langle\epsilon_r^q\rangle$ and $\langle\Omega_r^q\rangle$ as $\tau(q) \geq \mu(q)$. Since the longitudinal and transverse velocity increments can be thought of as being related to dissipation and enstrophy, respectively [15], it is conceivable that an analogous situation holds for velocity increments. This is an enticing prospect, since phenomenological models that are usually created for longitudinal increments, for instance [39, 40], can then be generalized to the velocity increment tensor in an uncomplicated manner.

Acknowledgements: We thank Theodore Drivas and Victor Yakhot for useful discussions. This work is partially supported by the National Science Foundation (NSF), via Grant No. ACI-1640771 at the Georgia Institute of Technology. The computations were performed using supercomputing resources provided through the XSEDE consortium (which is funded by NSF) at the Texas Advanced Computing Center at the University of Texas (Austin), and the Blue Waters Project at the National Center for Supercom-

puting Applications at the University of Illinois (Urbana-Champaign).

- [1] Harte J, Kinzig A and Green J 1999 *Science* **284** 334–336
- [2] Christensen K, Danon L, Scanlon T and Bak P 2002 *Proc. Nat. Acad. Sci.* **99** 2509–2513
- [3] Oboukhov A M 1962 *J. Fluid Mech.* **13** 77–81
- [4] Kolmogorov A N 1962 *J. Fluid Mech.* **13** 82–85
- [5] Stolovitzky G, Kailasnath P and Sreenivasan K R 1992 *Phys. Rev. Lett.* **69** 1178–1181
- [6] Joubaud S, Petrosyan A, Ciliberto S and Garnier N B 2008 *Phys. Rev. Lett.* **100** 180601
- [7] Bramwell S T 2009 *Nat Phys.* **5** 443 – 447
- [8] Sreenivasan K R and Antonia R A 1997 *Annu. Rev. Fluid Mech.* **29** 435–472
- [9] Schumacher J, Eckhardt B and Doering C R 2010 *Phys. Lett. A* **374** 861 – 865
- [10] Siggia E D 1981 *J. Fluid Mech.* **107** 375–406
- [11] Kerr R M 1985 *J. Fluid Mech.* **153** 31–58
- [12] Meneveau C, Sreenivasan K R, Kailasnath P and Fan M S 1990 *Phys. Rev. A* **41** 894–913
- [13] Brachet M 1991 *Fluid. Dyn. Res.* **8** 1–8
- [14] Chen S, Sreenivasan K R and Nelkin M 1997 *Phys. Rev. Lett.* **79** 1253–1256
- [15] Chen S, Sreenivasan K R, Nelkin M and Cao N 1997 *Phys. Rev. Lett.* **79** 2253–2256
- [16] Yeung P K, Sreenivasan K R and Pope S B 2018 *Phys. Rev. Fluids* **3** 064603
- [17] Nelkin M and Bell T L 1978 *Phys. Rev. A* **17** 363–369
- [18] He G, Chen S, Kraichnan R H, Zhang R and Zhou Y 1998 *Phys. Rev. Lett.* **81** 4636–4639
- [19] Nelkin M 1999 *Phys. Fluids* **11** 2202–2204
- [20] Donzis D A, Yeung P K and Sreenivasan K R 2008 *Phys. Fluids* **20** 045108
- [21] Yeung P K, Donzis D A and Sreenivasan K R 2012 *J. Fluid Mech.* **700** 5–15
- [22] Yeung P K, Zhai X M and Sreenivasan K R 2015 *Proc. Nat. Acad. Sci.* **112** 12633–12638
- [23] Siggia E 1981 *J. Fluid Mech.* **107** 375–406
- [24] She Z S, Jackson E and Orszag S A 1990 *Nature* **344** 226–228
- [25] Vincent A and Meneguzzi M 1991 *J. Fluid Mech.* **225** 1–20
- [26] Holzer M and Siggia E 1993 *Phys. Fluids* **5** 2525–2532
- [27] Pumir A 1994 *Phys. Fluids* **6** 2071–2083
- [28] Yakhot V 2003 *J. Fluid Mech.* **495** 135143
- [29] Donzis D A and Yeung P K 2010 *Physica D* **239** 1278–1287
- [30] Hamlington P E, Schumacher J and Dahm W J A 2008 *Phys. Rev. E* **77** 026303
- [31] Hamlington P E, Schumacher J and Dahm W J A 2008 *Phys. Fluids* **20** 111703
- [32] Kolmogorov A N 1941b *Dokl. Akad. Nauk. SSSR* **434** 16–18
- [33] Gotoh T and Fukayama D 2001 *Phys. Rev. Lett.* **86** 3775–3778
- [34] Ishihara T, Kaneda Y, Yokokawa M, Itakura K and Uno A 2003 *J. Phys. Soc. Jpn.* **72** 983–986
- [35] She Z S, Jackson E and Orszag S A 1990 *Nature* **344** 226 – 228
- [36] Douady S, Couder Y and Brachet M E 1991 *Phys. Rev. Lett.* **67** 983–986
- [37] Kambe T and Hatakeyama N 2000 *Fluid. Dyn. Res.* **27** 247 – 267
- [38] Frisch U 1995 *Turbulence* (Cambridge University Press)
- [39] Meneveau C and Sreenivasan K R 1987 *Phys. Rev. Lett.* **59** 1424–1427
- [40] She Z S and Leveque E 1994 *Phys. Rev. Lett.* **72** 336–339